Payri, R., Martí-Aldaraví, P., Quintero, P. M., Marco-Gimeno, J. (2021). Large Eddy Simulation for the Prediction of Human Coughing. In Atomization and Sprays. https://doi.org/10.1615/atomizspr.2021037129

Atomization and Sprays, 31(9):49–73 (2021)

LARGE EDDY SIMULATION FOR THE PREDICTION OF HUMAN COUGHING

Raúl Payri, Pedro Martí-Aldaraví,* Pedro M. Quintero, & Javier Marco-Gimeno

CMT-Motores Térmicos, Universitat Politècnica de València, València, Spain

*Address all correspondence to: Pedro Martí-Aldaraví, CMT-Motores Térmicos, Universitat Politècnica de València, València, Spain, E-mail: pedmar15@mot.upv.es

Original Manuscript Submitted: 11/17/2020; Final Draft Received: 5/9/2021

The health awareness that has arisen from the COVID pandemic has been translated into interest in studying the contagion methods of airborne viruses. The cough mechanism is one cause of virion spread. To analyze this phenomenon, computational fluid dynamics (CFD) simulations of the human cough have been set up in closed room conditions. Fundamental droplet, air, and thermodynamic conditions for the problem have been extracted from the literature and applied to the simulations performed. Three typologies of cough have been computed corresponding to the maximum, minimum, and mean peak cough velocities of the human being, and their corresponding injection profiles. Coughs were simulated in transient conditions and the droplets were tracked following an Eulerian-Lagrangian approach and large eddy simulation (LES) formulation for the turbulence phenomenon. Results revealed droplet travel distances of almost 2 m for the strongest cough case. Also, the presence of droplets smaller than 5 μm of diameter, the main virus spreader, was considerably larger than particles of bigger size. Additionally, most of the droplets evaporate or fall to the ground within 2 s after their injection. The remaining ones that stayed above the waistline or remained suspended in the air followed trajectories coming from buoyancy effects rather than being driven by the initial velocity profile. Moreover, it was found how almost the totality of the droplets expelled followed a trajectory towards the floor. Droplets that did not evaporate during the fluid injection became airborne for at least 5 seconds after the coughing.

KEY WORDS: *COVID-19, cough, droplets, CFD, PDF, trajectories, aerosols*

1. INTRODUCTION

The spread during 2020 of the Severe Acute Respiratory Syndrome CoronaVirus 2 (SARS-CoV-2) around the globe has caused the need of acquiring knowledge about ways of transmission of respiratory infections. Coughing or sneezing expels many droplets capable of spreading the virus (Tang et al., 2006). The SARS-like virus has a Reproductive Factor (R0) of 2–3 (Lipsitch et al., 2003) indicating the importance of the transmission via airborne nuclei or droplets. Speaking, coughing, and sneezing produce very many droplets small enough to remain airborne as droplet-nuclei. Nearly all of these small droplets originate from the front of the mouth; only relatively few, if any, originate from the nose, as in sneezing and breathing, or from the throat, as in sneezing, coughing, speaking, and laughing as stated by Duguid (1945). In the mentioned investigation it was found that when a cough was performed with the mouth kept well open and the tongue depressed ("throat-only cough"), few or no droplets were expelled; when, on the

Payri, R., Martí-Aldaraví, P., Quintero, P. M., Marco-Gimeno, J. (2021). Large Eddy Simulation for the Prediction of Human Coughing. In Atomization and Sprays. https://doi.org/10.1615/atomizspr.2021037129

other hand, the mouth was closed at the start of the cough, either by approximation of the lips ("lip cough") or by approximation of the tongue and teeth ("tongue-teeth cough"), many droplets were expelled.

There was no great difference between the size distributions of the droplet-nuclei produced by the different types of expiratory activity; in general, smaller nuclei were produced in the more "violent" activities, especially in sneezing (Duguid, 1946). Speaking generates less than an order of magnitude smaller number of droplets (250) than coughing (5000) and sneezing (1,000,000) (Duguid, 1946). The number of droplets expelled during a sneezing event suffers from great variation between studies, as Cole and Cook (1998) report values up to 40,000 particles. Variation for average droplet size among the three age groups was insignificant. Moreover, the variation in average droplet size between males and females was also insignificant. While the variation in droplet concentration between males and females was significant, being higher for male subjects due to the increased flow rate compared to female test subjects (Yang et al., 2007).

Expelled droplets are not the same as droplet-nuclei or even bacteria-carrying droplet-nuclei. Duguid (1945) clearly differentiates them, which is important when studying the illness transmission. In speaking about a particular illness transmission system, knowing the origin of expelled droplets (mouth, nose, lung, respiratory tract, etc.) plays a major role. Gupta et al. (2009) reviewed the available data about coughing with the goal of establishing the proper computational fluid dynamics (CFD) boundary conditions for a cough simulation. The data required were the flow rate, spray direction, spray angle, the open area of the mouth, the cough temperature, and the virus droplets' size distribution. Zhu et al. (2006) agrees on the importance of establishing proper boundary conditions. According to them, temperature and size distribution of droplets were well characterized in the literature, so their work focused on measuring flow rates, flow directions (and cough spray cone angles, which are clearly not axis-symmetric), and mouth opening of coughs. In fact, their literature review led them to conclude that the measurements of the flow rate and direction must be performed with a frequency of 100 Hz or higher.

Following the results of Redrow et al. (2011), remarkable distribution was due to turbulent diffusion rather than forced convection of the continuous phase (air). This pattern was repeated for inhomogeneous turbulent diffusion.

Gupta et al. (2009) also comment and prove the large variability of characteristic cough parameters. They conclude that the cough flow characteristics from a subject cannot be used to represent the whole population, which means a standard cough does not exist. Considerable subject variability was observed also by Xie et al. (2009) who studied the droplet size distribution of expiratory activities. Following this idea, Aliabadi et al. (2010) say that there is no unique droplet size distribution associated with coughs and sneezes. This is due to the inherent physiological variability in different subjects. Therefore, a distribution must be assumed that covers a wide range of droplet sizes with a representative mean.

The violence of coughs would be different for patients with respiratory diseases and thus has an effect on droplet generation, as well as more secretions of fluids on airway surfaces and higher frequency of coughing (Papineni and Rosenthal, 1997; Xie et al., 2009). As mentioned by Bourouiba et al. (2014) violent respiratory events release droplet-bearing turbulent momentum puffs of moist, buoyant air ejected in a direction that depends on the individual.

The particle sizes expelled by a cough cover a wide range. Gupta et al. (2009) say the droplet diameter range falls within 1–10 μm, while Xie et al. (2009) conclude that the maximum size range is about 50–100 μm. Their experiment allowed them to measure particle diameters larger than 0.5 μm. An average of 800 droplets could be observed from 20 coughs. About 2.5% of the droplets were less than 20 μm and 1.4% less than 10 mm. Only 20% of the droplets were

Payri, R., Martí-Aldaraví, P., Quintero, P. M., Marco-Gimeno, J. (2021). Large Eddy Simulation for the Prediction of Human Coughing. In Atomization and Sprays. https://doi.org/10.1615/atomizspr.2021037129

less than 50 mm and 64% of the droplets less than 100 mm. Nevertheless, Xie et al. (2009) conclude that it is not enough to know the size distribution of droplets detected on sampling slides, which is not the real size distribution of droplets generated during expiratory activities. Additionally, they state that droplets smaller than 47 μm in diameter in origin evaporate before they reach the sampling surface, so they are not accounted for in the study. When the droplet diameter at the origin is larger than 80 mm, droplet size changes very little. As mentioned in Loudon and Roberts (1967), many factors have effects on the numbers of droplets, such as the amount of secretion present in the mouth and its location, and the placement and movement of lips, tongue, and teeth during the cough. The significance of droplet size is noted by Redrow et al. (2011), stating that particles with a diameter of less than 10 μm remain suspended for enough time to disperse throughout the room. Larger droplets are removed from the air more rapidly by gravitational settling. According to Redrow et al. (2011), up to 3000 droplets can end up as airborne particles.

Apparently, convection flows due to body heat may play a role in the droplet dispersion according to Zhu et al. (2006) as they induce ascending streams around the human body, so a detailed modeling of the external anatomy is recommended for numerical analysis.

Zhu et al. (2006) also performed CFD analysis of coughing for several situations but always with air conditioning on—a standard office and a standard bedroom, with two subjects in them, with different relative positioning. Constant velocity was assumed for both coughing and breathing processes of the subjects. They do realize the importance of social distancing but also the positioning of the air conditioning device for closed environments.

Evaporation of droplets needs to be considered and the process is highly affected by the ambient relative humidity. Additionally, the employed evaporation model and droplet composition will play a significant role in the results according to Redrow et al. (2011), who developed a multicomponent evaporation model for coughing liquid phase.

Thus, the aim of this study is to predict the main characteristics of the human cough by using CFD methodology in closed room conditions. Three different cough typologies will be simulated representing the whole range of typical human coughs. Large eddy simulation (LES) mesh quality requirements are to be assessed. From them, information of cough dispersion and penetration shall be obtained, as well as possible airborne droplet detection and their trajectories around the gaseous domain. Due to the existing doubts of which particles are the disease transmitting droplets, the analysis performed will report on how the cough sprays develop, and how the droplets disperse around the surrounding air, which will help understand how the pathogens can travel around.

This document is presented in four sections as follows. This section, the introduction, is where the need for this study is presented, as well as the main findings obtained by other studies regarding human coughs. It is followed by a literature review section in which the main boundary conditions for the CFD simulations will be obtained. Later, the results coming from the three cases calculated are presented, analyzing parameters such as penetration, Sauter mean diameter evolution, and trajectories calculated for the expelled droplets. A conclusions section closes up with the main obtained findings.

2. COMPUTATIONAL METHODOLOGY

2.1 Geometry and Mesh

The geometry model used for the simulations is the same as the one used by other researchers (Feng et al., 2020; Zhao et al., 2019). It consists of a human geometry, of 1.80 m in height. It

Payri, R., Martí-Aldaraví, P., Quintero, P. M., Marco-Gimeno, J. (2021). Large Eddy Simulation for the Prediction of Human Coughing. In Atomization and Sprays. https://doi.org/10.1615/atomizspr.2021037129

was placed within a room of 5 m (x-direction) by 3 m (y-direction) by 5.7 m (z-direction). The human body is located at 0.7 m from the back wall. There is enough space for the cough jet to develop and for the corresponding puff to move afterwards without influence of the boundaries of the room.

Gupta et al. (2009) reported constant mouth area during cough, and an average value of 4.00 ± 0.95 cm^2 for male subjects and 3.37 ± 1.40 cm^2 for female. In accordance with these results, the diameter of the mouth of the mannequin is 0.01905 m (area of 2.85 cm^2) for the simulations of Redrow et al. (2011), 0.0217 m (area of 3.70 cm^2) for those of Dudalski et al. (2020), and 0.020 m (area of 3.14 cm^2) for those of Li et al. (2018) and Aliabadi et al. (2010). Additionally, Bourouiba et al. (2014) estimated the area to be 3.4 cm^2 during the cough. Mouth shape is also of importance. Dbouk and Drikakis (2020) reported a rectangular-like mouth with an aspect ratio of 8.26. Yang et al. (2018) also followed the same procedure. For that, the mouth of the human model used for the present study has been modified to an ellipsoidal shape, with an area of 3.4 cm^2 and an aspect ratio of 8.26 (major semiaxis of 2.99 cm and minor semiaxis of 0.362 cm).

The base grid size is 100 mm. Cells next to the body are also refined, with three levels for the body torso and limbs, and five levels for the cells surrounding the head. The semitransparent blue cone shown in Fig. 1 represents the volume with five levels of refinement (each cell is divided into $2^5 = 32$ smaller cells). With this cell configuration, the cell count achieved for the later simulations is 13 million. All boundaries of the domain, including the body surface, are considered stationary nonslip walls with constant temperature (different values for the room and for the body) except one, the one representing the mouth, which can also be seen in the close-up of Fig. 1.

2.2 Cough Jet Conditions

Following the requirements established by Zhu et al. (2006), cough flow rate and direction are other parameters of critical importance for accurate simulations. The boundary conditions and flow rate profiles differ between the researchers. On the one hand, studies like Zhao et al. (2005),

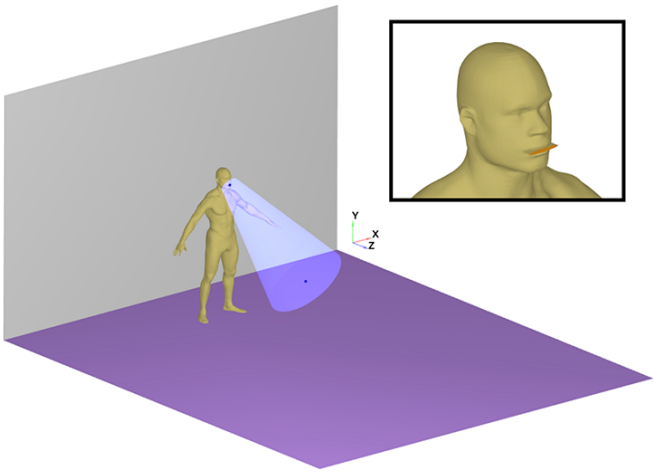

FIG. 1: Computational domain and mesh refinement region

Payri, R., Martí-Aldaraví, P., Quintero, P. M., Marco-Gimeno, J. (2021). Large Eddy Simulation for the Prediction of Human Coughing. In Atomization and Sprays. https://doi.org/10.1615/atomizspr.2021037129

Zhu et al. (2006), and Gao et al. (2008) selected a constant flow speed value during 0.5 s. On the other hand, Gupta et al. (2009) expressed a flow-rate time-varying profile according to three characteristic parameters (which are gender, height, and weight dependent): cough peak flow rate (CPFR), cough expired volume (CEV), and peak velocity time (PVT). All these parameters are linked with a mathematical expression [Eqs. (1) and (2)] to fit their experimental results. The limits of the parameters reported in the literature are summarized in Table 1. Another study that used a time-varying profile was performed in Redrow et al. (2011). It is compared in Fig. 2 against the one the present study has used to see that there are no great differences between the profiles.

$$\bar{M} = \frac{a_1 \tau^{b-1} \exp\left(-\tau/c_1\right)}{\Gamma\left(b_1\right) c_1^{b_1}} \quad \text{for} \quad \tau < 1.2, \tag{1}$$

$$\bar{M} = \frac{a_1 \tau^{b-1} \exp\left(-\tau/c_1\right)}{\Gamma\left(b_1\right) c_1^{(b_1)}} + \frac{a_2 \left(\tau - 1.2\right)^{(b_2-1)} \exp\left(-\left(\tau - 1.2\right)/c_2\right)}{\Gamma\left(b_2\right) c_2^{b_2}} \quad \text{for} \quad \tau > 1.2, \tag{2}$$

where

- $\overline{M} = FlowRate/CPFR$,
- $\tau = Time/PVT$,
- $a_1 = 1.680$,

TABLE 1: Reported limits of cough flow parameters

	Male		**Female**	
	Min.	**Max.**	**Min.**	**Max.**
CPFR (L/s)	3	8.5	1.6	6
CEV (L)	0.4	1.6	0.25	1.25
PVT (ms)	57	96	57	110

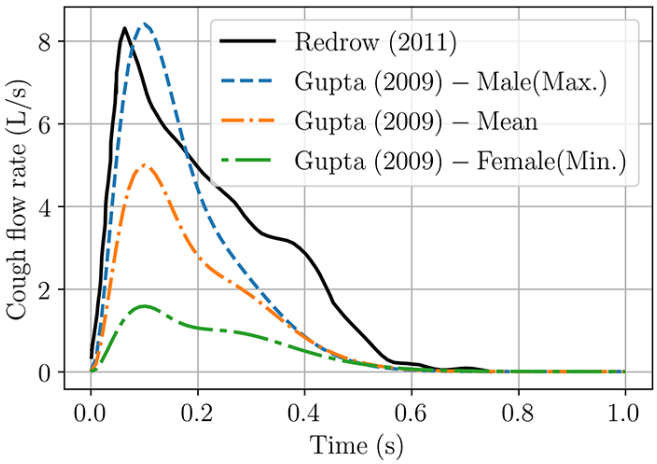

FIG. 2: Reported time-varying flow rate of coughing

Payri, R., Martí-Aldaraví, P., Quintero, P. M., Marco-Gimeno, J. (2021). Large Eddy Simulation for the Prediction of Human Coughing. In Atomization and Sprays. https://doi.org/10.1615/atomizspr.2021037129

- $b_1 = 3.338$,
- $c_1 = 0.428$,
- $a_2 = CEV/(PVT \times CPFR) - a_1$,
- $b_2 = (-2.158 \times CEV)/(PVT \times CPFR) + 10.457$,
- $c_2 = 1.8/(b_2 - 1)$.

For this study, the mathematical expression of Gupta et al. (2009) has been employed. Three different profiles have been introduced according to the maximum, mean, and minimum data of the CEV, CPFR, and PVT reported (Table 1). Regarding the direction of the exhalation, Zhao et al. (2005) assumed it to be 30° downward. Bourouiba et al. (2014) reported an inclination angle of $24 \pm 7°$, and Gupta et al. (2009) reported an angle of $27.5 \pm 5°$. With this information, a downward direction of 30° has been selected for the present study. When it comes to the spray angle, Gupta et al. (2009) presented an initial spray angle of $25 \pm 5°$; these results were confirmed by Tang et al. (2009). Therefore, a spray cone angle of 25° is chosen. The expelled air temperature has been set accordingly to Eq. (3), with $R = 98.12\%$, obtained from the data presented by Höppe (1981). The liquid mass expelled at coughing was set as the mean value reported by several previous studies. These values are presented in Table 2, which leads to a total mass of 3.6 mg of water droplets expelled during the duration of the cough.

$$T_{exp} = 0.1976 \cdot (T_a - 273) + 302.9685. \tag{3}$$

Another aspect of importance is the droplet size distribution needed to introduce a representative spray during the simulations as noted in the Introduction section. Studies report a great variability when obtaining this information due to the wide range of methodologies employed. A summary is included in Fig. 3. From the dataset presented, the Chao et al. (2009) droplet size distribution has been selected as another researcher (Li et al., 2018) has already used it, and agreement between the two studies was found. Two probability distribution fittings were performed with Rosin-Rammler and chi-squared shaped curves on the mentioned data. Results of this fitting are included in Fig. 4, from which the Rosin–Rammler curve has been selected, which corresponds to a shape parameter of value 2.7 and a scale parameter of 10 μm.

When it comes to the ambient conditions, the ambient temperature and relative humidity of the air have been set to be 296 K and 60%, respectively, according to acceptable values of the Spanish *Real Decreto 107/2007*, according to the *Law 31/1995* for representative values throughout the whole year. The spray injection profile has been simulated for three different

TABLE 2: Summary of the cough saliva total mass measurement results

Reference	Method	Subjects	Mass (mg)
Zhu et al. (2006)	Mask	3	6.70 ± 0.8
Xie et al. (2009)	Mask	5	1.15 ± 0.8
Xie et al. (2009)	Bag	9	4.25 ± 1.7
Zayas et al. (2012)	Laser diffraction	45	2.2

Payri, R., Martí-Aldaraví, P., Quintero, P. M., Marco-Gimeno, J. (2021). Large Eddy Simulation for the Prediction of Human Coughing. In Atomization and Sprays. https://doi.org/10.1615/atomizspr.2021037129

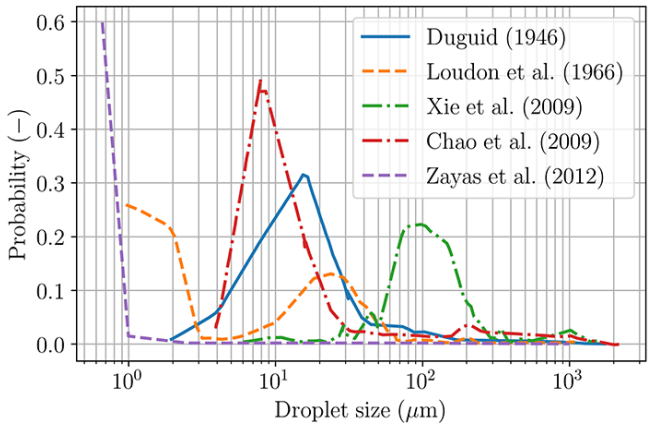

FIG. 3: Reported probability droplet size distribution of coughing

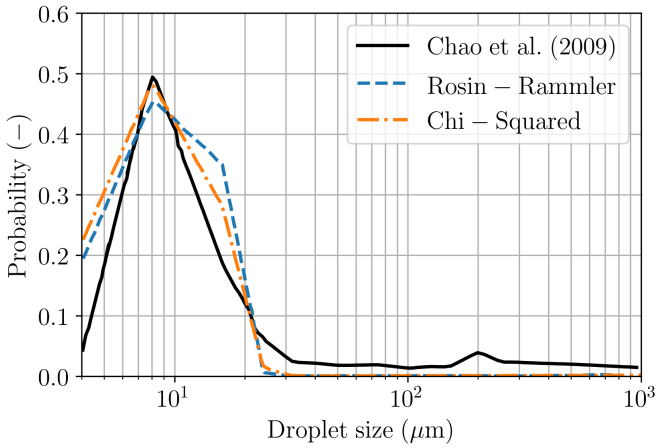

FIG. 4: Computational domain and mesh refinement region

cases, according to the cough inlet profile range introduced by Gupta et al. (2009), and correspond to the curves of Fig. 2. Zero-gradient has been set for the body surface, while 310 K has been set for the temperature. Referring to the ambient conditions, a value of 101,325 Pa has been established, and a temperature of 296 K, a value which has been later introduced into Eq. (3). A summary of the boundary conditions for the simulations performed is included in Table 3.

2.3 Governing Equations

The software employed to simulate the different coughs is CONVERGE 2.4. In order to simulate the air and saliva [water, according to Gittings et al. (2015)] droplet movements, an Eulerian-Lagrangian approach is employed, the air being the carrier phase under the Eulerian framework and the saliva the discrete phase resolved by means of the Lagrangian method. This approach is also known as discrete phase modeling (DPM) or discrete droplet modeling (DDM). For the carrier phase, the species [Eq. (4)], continuity [Eq. (5)], momentum [Eq. (6)], where σ_{ij} is the

Payri, R., Martí-Aldaraví, P., Quintero, P. M., Marco-Gimeno, J. (2021). Large Eddy Simulation for the Prediction of Human Coughing. In Atomization and Sprays. https://doi.org/10.1615/atomizspr.2021037129

TABLE 3: Cough jet boundary conditions

Parameter	Value
Mass flow inlet	Max-mean-min velocity profiles (Gupta et al., 2009)
Injection profile	Normalized max-mean-min velocity profiles (Gupta et al., 2009)
Droplet distribution	RR fitting with Chao et al. (2009) data
Temperature	307.9 K
Fluid injected	Water
Spray orientation	30° downward
Spray cone angle	25°

viscous stress tensor) and energy [Eq. (7)] transport equations are utilized in a PISO (pressure-implicit with splitting of operators) framework (Weller et al., 1998). In these equations, S represents the corresponding source term.

$$\frac{\partial \rho_m}{\partial t} + \frac{\partial \left(\rho_m \, u_j\right)}{\partial x_j} = \frac{\partial}{\partial x_j}\left(\rho \, D \, \frac{\partial Y_m}{\partial x_j}\right) + S_m \;\; \text{where} \;\; \rho_m = Y_m \, \rho, \tag{4}$$

$$\frac{\partial \rho}{\partial t} + \frac{\partial \left(\rho \, u_i\right)}{\partial x_i} = S, \tag{5}$$

$$\frac{\partial \left(\rho \, u_i\right)}{\partial t} + \frac{\partial \left(\rho \, u_i \, u_j\right)}{\partial x_i} = -\frac{\partial P}{\partial x_i} + \frac{\partial \sigma_{ij}}{\partial x_j} + S_i, \tag{6}$$

$$\begin{aligned} \frac{\partial \left(\rho \, e\right)}{\partial t} + \frac{\partial \left(\rho \, e \, u_j\right)}{\partial x_i} &= -P\frac{\partial u_j}{\partial x_j} + \sigma_{ij}\frac{\partial u_i}{\partial x_j} \\ &\quad + \frac{\partial}{\partial x_j}\left(K \, \frac{\partial T}{\partial x_j}\right) + \frac{\partial}{\partial x_j}\left(\rho \, D \, \sum_m h_m \, \frac{\partial Y_m}{\partial x_j}\right) + S. \end{aligned} \tag{7}$$

On the other hand, the equation of motion of each parcel [Eq. (8), where u_i' is the fluctuating gas velocity and r_p is the parcel radius] allows us to obtain its velocity, v_i, and so its trajectory or position.

$$\frac{\mathrm{d}v_i}{\mathrm{d}t} = \frac{3}{8}\,\frac{\rho}{\rho_l}\,C_D\,\frac{|u_i + u_i' - v_i|}{r_p}\,(u_i + u_i' - v_i) + g_i. \tag{8}$$

The complete set of transport equations (in a conservative form) is implicitly solved in a PISO loop, with two to nine iterations until is reached a tolerance of 10^{-3}. A successive over-relaxation (SOR) linear solver is used for all transport equations. A tolerance of 10^{-5} is selected for the momentum equation, 10^{-8} for the pressure corrector, and 10^{-4} for the rest of the equations. No under-relaxation factors were used. A reconstructed second-order central difference method is used for spatial discretization. A first-order Euler time scheme is employed, being the time step selected in order to get a maximum Courant-Friedrichs-Levy (CFL) number of 1.0.

2.4 Computational Submodels

Several submodels are needed in the present simulations. The turbulence modeling is one of the most relevant because it affects the mixing and coalescence of particles and droplets (Bourouiba

Payri, R., Martí-Aldaraví, P., Quintero, P. M., Marco-Gimeno, J. (2021). Large Eddy Simulation for the Prediction of Human Coughing. In Atomization and Sprays. https://doi.org/10.1615/atomizspr.2021037129

et al., 2014). The LES approach is selected so large scales of turbulence are solved while small ones are modeled through a subgrid scale (SGS) model. The filter employed to select large and small scales is the grid itself. The SGS model utilized is the dynamic Smagorinsky model (DSM), a zero-dimensional model which relates the turbulent viscosity to the magnitude of the strain tensor and cell size by means of a proportionality constant which depends on the local regime of the flow (Germano et al., 1991). This SGS model capabilities for calculating the Smagorinsky constant has been considered to be useful due to the variation of flow and droplet velocities that can be found in the spray region.

Another important submodel is the droplet injection one. According to Duguid (1945) observations, air velocities are high enough for atomization to occur when the breath is forced out through some part of the respiratory tract. Tongues of liquid are drawn out from the surface, pulled thin, and broken into columns of droplets before exiting the mouth. Additionally, Bourouiba et al. (2014) show that the common assumption of the punctual droplet source may not be correct for a cough. Therefore, a solid cone injection model is used, with an exit circular section with 3.4 cm^2 area and an opening angle of 25°. The injected droplet size follows a Rosin-Rammler distribution, as explained in Section 2.2, being introduced into the computational domain with a velocity directly (without using a discharge coefficient model) established from the cough flow rate defined by Gupta et al. (2009) (see Section 2.2).

After being expelled, droplets might be subject to several processes. For instance, they exchange momentum with the surrounding air (liquid/gas coupling). Thus, a droplet drag model is necessary to accurately model the spray evolution. In these simulations, the droplet drag coefficient is determined dynamically, accounting for variations in the drop shape through a drop distortion parameter (Liu et al., 1993). Droplets can also interact between them, colliding, with different outcomes (rebounds and/or coalescence). The no time counter (NTC) collision method of Schmidt and Rutland (2000) is used to account for that. This submodel is directly derived from the basic probability model for stochastic collision, proving to be faster and more accurate than other alternatives (under certain conditions).

Saliva droplets may also gradually evaporate, reducing their size and finally leaving behind their nonvolatile components. Although multicomponent evaporation models are available in the literature (Li et al., 2018), that is not the case in the present study, where saliva droplets are made of only water. Then, the correlation from Frössling (1940) is selected for determining the time rate of change of the droplet size, assuming constant droplet temperature (the hypothesis is used to compute the heat exchange with the surrounding air). Finally, droplet diameter can be also diminished due to the atomization phenomenon. This has been taken into account by using Kelvin-Helmholtz (KH), for primary breakup, and Rayleigh-Taylor (RT), for secondary breakup (Beale and Reitz, 1999). For these submodels (but also the others), values of the characteristic constants are presented in Table 4. The simulation was performed on 64 Intel Xeon Gold 6154 cores. A maximum of 3 GB per core was needed, and the simulation was run for 4.5 s of simulated time, and a computational cost of 4600 CPU-h.

2.5 Mesh Quality Assessment

The element size during LES directly controls which scales of the turbulent flow are resolved, and which of them are modeled. It acts as a filter for this purpose. The largest scales should be fully resolved, while the smallest ones should be filtered out. A good LES should resolve enough turbulent structures and, generally, it is assessed through a quality index. Pope (2004) introduces a quality index based on an activity parameter s which takes into account the turbulent

Payri, R., Martí-Aldaraví, P., Quintero, P. M., Marco-Gimeno, J. (2021). Large Eddy Simulation for the Prediction of Human Coughing. In Atomization and Sprays. https://doi.org/10.1615/atomizspr.2021037129

TABLE 4: KH-RT model constants

Parameter	Value
KH fraction of injected mass/parcel	0.05
KH shed mass constant	1
KH model size constant	0.61
KH model velocity constant	0.188
KH model breakup time constant	7
RT breakup time constant	1
RT model size constant	0.1

viscosity and the numerical dissipation ν_{num} [Eq. (9)]. The proposed quality index takes the shape of Eq. (10), where α_ν and n are model constants. The quality index has been computed for a time instant where the cough event was almost finished. Figure 5 shows the results of this computation, by restraining the values above acceptable quality values ($> 80\%$). It is notable to see how the lowest quality achieved (0.66) is in the immediate zones around the human body, where there is a sudden cell growth from the cough cone embedding to the base cell size which is considerably large (0.26 m). The region of interest, within which the main spray should be lying, as it does have a considerable smaller cell size, reaches a higher quality, almost 1, except for the effects of the turbulence during the spray injection, which lowers this value to approximately 0.9, which is an acceptable value. Therefore, the proposed mesh has been carried forward to simulate the cough dynamics proposed.

$$s^* = \frac{\langle \nu_t \rangle + \langle \nu_{num} \rangle}{\langle \nu_t \rangle + \langle \nu_{num} \rangle + \nu}, \tag{9}$$

$$IQ_\nu = \frac{1}{1 + \alpha_\nu \left(\dfrac{s^*}{1 - s^*} \right)^n}. \tag{10}$$

3. RESULTS

3.1 Validation Data

Unfortunately, to the best of the authors' knowledge, there is not a complete description of a coughing event available in the literature. This means that the amount of saliva expelled, the droplet size distribution, the exhaled air mass flow information, droplet residence time, and traveled distance data are never provided for the same individual (or group of persons). This makes a direct and quantitative validation of the simulations not possible. Instead, simulation results are checked to fall within the range of several parameters provided by the different researchers.

In the analysis of the spray penetration of a cough [which could be larger than 2 m (Zhu et al., 2006)], Bourouiba et al. (2014) found two different phases. The first one was dominated by a jetlike dynamics ($S\left(t\right) \propto t^{1/2}$) with a duration similar to that of the cough, and the second one by a pufflike dynamics ($S\left(t\right) \propto t^{1/4}$), which lasts until ~ 35 s.

For this study, the penetration of the saliva droplets is calculated to know how far the particles can reach. In each time step, the total mass injected is calculated and multiplied by the liquid

Payri, R., Martí-Aldaraví, P., Quintero, P. M., Marco-Gimeno, J. (2021). Large Eddy Simulation for the Prediction of Human Coughing. In Atomization and Sprays. https://doi.org/10.1615/atomizspr.2021037129

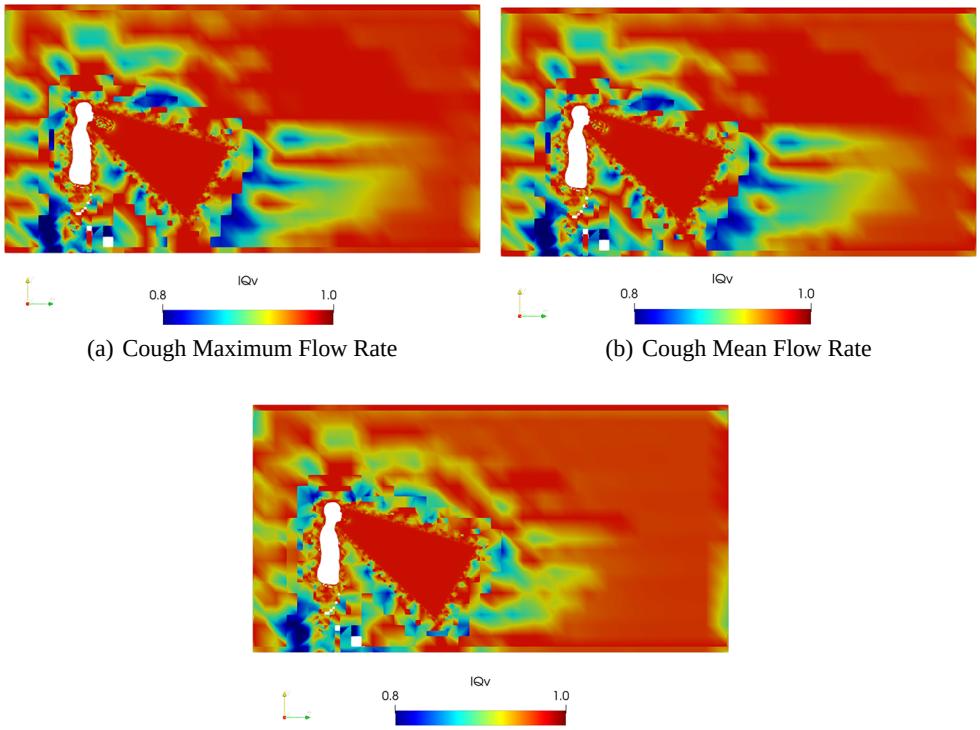

(a) Cough Maximum Flow Rate

(b) Cough Mean Flow Rate

(c) Cough Minimum Flow Rate

FIG. 5: Viscosity quality index contour for the three simulations performed at the time of maximum flow rate (0.1 s)

penetration fraction, which in this case has been decided to be 99%, giving the penetrated spray mass, whose distance towards the mouth returns the wanted penetration. This is performed for each one of the three simulations, at maximum, mean, and minimum flow rate profiles. Figure 6 shows the results of the explained procedure. Two phases can be distinguished from it as stated by Bourouiba et al. (2014), whose transition occurs at 0.5 s. A fitting has been made for each of the two phases to analyze if they had the same tendencies as stated by Bourouiba et al. (2014), the first one $S(t) \propto t^{1/2}$, and $S(t) \propto t^{1/4}$ for the second one. These fittings are shown in Fig. 7. The mathematical expressions are included within the plot, and they yield a R^2 coefficient of 0.976 for the fitting of the first phase and 0.985 for the fitting of the second phase. In any of the three simulations there is enough evidence to say that as the penetrations are progressively increasing, there are a certain amount of droplets that remain airborne, as if they had fallen to the ground; the curves should have stabilized at a specific value. By normalizing the previous results and presenting them in a logarithmic way, the three coughs injected mostly collapse to one curve up to a nondimensional time of 100. In addition to that, it exhibits a linear behavior from nondimensional time 10 to nondimensional time 100, as presented by Liu and Novoselac (2014), which contributes to the idea of a power relationship with time. The change of phase can also be seen in this later plot. When the curves penetration curves change their dependency with time to $S(t) \propto t^{1/4}$, the slope of the logarithmic plot has also changed in Fig. 6(b).

Payri, R., Martí-Aldaraví, P., Quintero, P. M., Marco-Gimeno, J. (2021). Large Eddy Simulation for the Prediction of Human Coughing. In Atomization and Sprays. https://doi.org/10.1615/atomizspr.2021037129

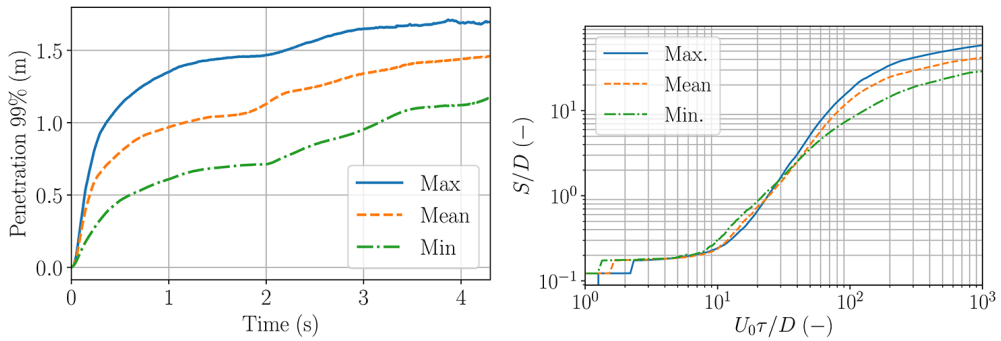

(a) Penetration with time (b) Non-dimensional penetration with time

FIG. 6: Cough penetration, and Logarithmic non dimensional penetration for the three simulations performed

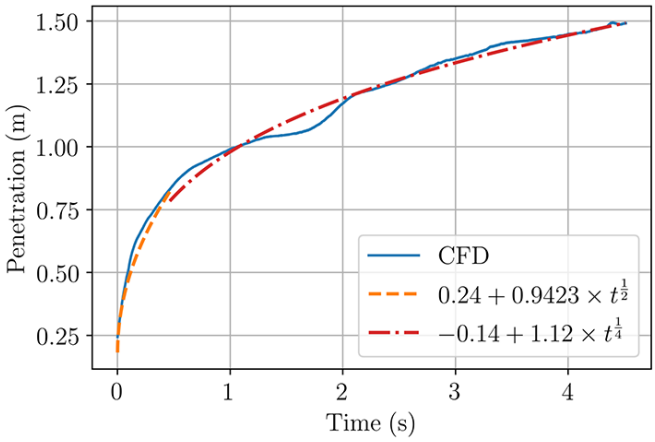

FIG. 7: CFD data with fitting data for the two phases of the mean flow rate profile

Loudon and Roberts (1967) report how the total number of droplets are distributed in different sections of a box of 0.366 m × 0.508 m × 0.305 m, the mouth being located at an entry port at about two-thirds of the height of the wall at one end of the box. This box is sketched in Fig. 8, together with their results [Fig. 8(a)]. It was found that 60% of the droplets did go to the ground in a distributed way, 30% of the particles did reach the back wall, and the remaining droplets impacted in the lateral wall. The same box was built by Xie et al. (2009), who divided it in even more sections [see Fig. 8(b)]; they found that 81% of the droplets were deposited on the base of the box, evenly distributed, and 15% of them could reach the back wall.

In order to predict the trajectories of the droplets exhaled during the cough, a similar study has been done. A virtual box of identical dimension of these two studies has been created (502 × 305 × 366 mm). All the saved time steps for the three simulations have been processed, and it has been determined when a droplet has intersected with the virtual parallelepiped. This box is also discretized in the same regions as that of Xie et al. (2009) to obtain where the droplets intersect with it. The orientation angle at which the cough is injected is not clear from the studies of Xie et al. (2009) and Loudon and Roberts (1967); therefore, the virtual box has been rotated

Payri, R., Martí-Aldaraví, P., Quintero, P. M., Marco-Gimeno, J. (2021). Large Eddy Simulation for the Prediction of Human Coughing. In Atomization and Sprays. https://doi.org/10.1615/atomizspr.2021037129

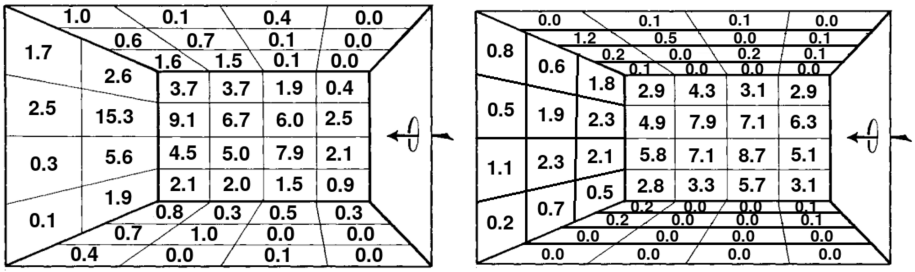

(a) Loudon and Roberts (1967) data. (b) Xie et al. (2009) data.

FIG. 8: Site of recovery of droplets after coughing. Numbers represent percentage of droplets recovered.

30° to match the spray injection angle. Figure 9 shows the result of this procedure. Ninety percent of the droplets fall to the ground in the maximum flow rate profile [Fig. 9(a)], and the remaining droplets reach the back wall. The same percentage of droplets fall to the ground in the mean profile [Fig. 9(b)], but the floor distribution is displaced towards the cough inlet. The total amount of droplets expelled intersect with the box bottom for the weakest cough simulated [Fig. 9(c)], and the distribution is moved even more towards the domain inlet. In all three cases, the droplets detected are not evenly distributed around the box vertical symmetry plane (X-Y plane according to Fig. 1), as there is a trend towards the left side of the box (negative X values

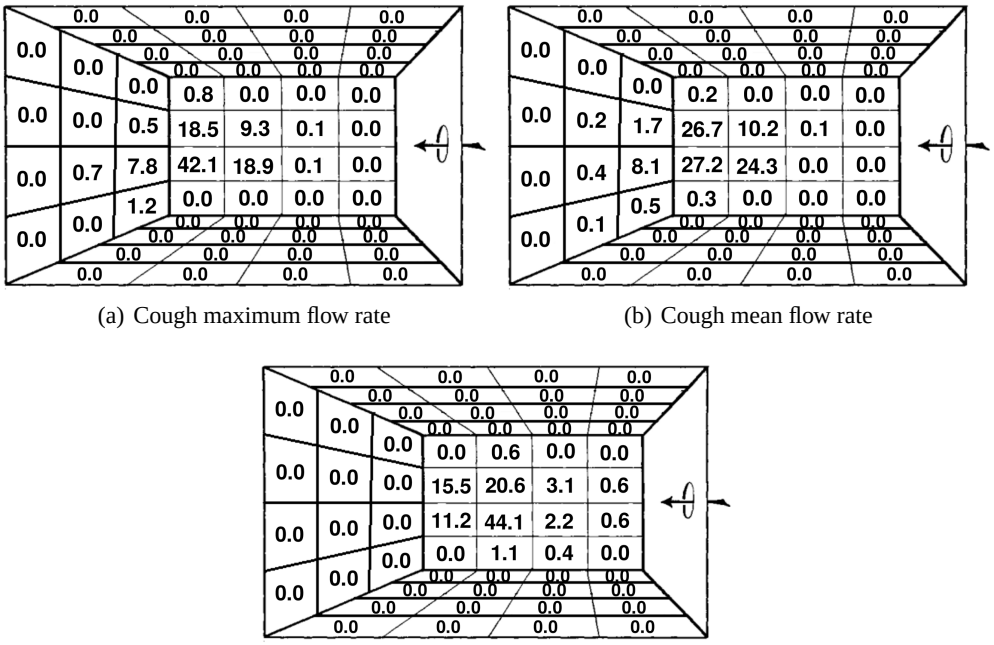

(a) Cough maximum flow rate (b) Cough mean flow rate

(c) Cough minimum flow rate

FIG. 9: Droplet recovery sites inside a box of 502 × 305 × 366 mm. Numbers in percentage of total droplets.

Payri, R., Martí-Aldaraví, P., Quintero, P. M., Marco-Gimeno, J. (2021). Large Eddy Simulation for the Prediction of Human Coughing. In Atomization and Sprays. https://doi.org/10.1615/atomizspr.2021037129

according to the axis of Fig. 1). No particle is found to cross the box sidewalls. Although the amount of droplets that fall to the ground differs between CFD data and the results from Loudon and Roberts (1967), it shows good agreement with the Xie et al. (2009) outcomes, with an error of 10% on the amount of droplets that reach the back wall and ground, and all of them agree that almost no particles impact on the sidewalls, which shows the reasonableness of the computational method.

The validation has been completed using the data coming from Morawska (2006), which include the time it takes for the droplets to fall 1 m after being injected. According to them, it takes 300 s for the droplets of 10 μm of diameter, and 30,000 s for the droplets of 1 μm. In the CFD results, from the droplets that remain in the air once the simulation has finished (4 s), whose maximum diameter is of 25 μm (Section 2.2), the 90% have not fallen 1 m vertically from the injection point (the mouth).

3.2 SMD Evolution

The evolution of the cough droplet size has been assessed through a characteristic diameter. SMD has been chosen for it, as it represents the ratio of volume to surface area of the spray. Results are included in Fig. 10. There is a quick rise of the SMD in the first simulation instants, as droplets are being introduced into the domain. In general terms, after 0.2 s the curve tends to a specific value as the small water droplets, which have a shorter lifetime, are evaporating into the gas, while the bigger droplets, with a longer lifetime, remain in the domain. Once the aerodynamic drag has slowed down the droplets, the convective effects on the evaporation are less important and therefore the SMD reaches a stationary value. The three coughs tend to reach almost the same asymptote of 15 μm. As the injection duration of each of the profiles changes (0.5, 0.6, and 0.9 s for the minimum, mean, and maximum peak flow rate profiles), the SMD curves change as well. The minimum peak flow rate profile tends to the asymptote value sooner as the injection event is the shortest of the three profiles. Also, the low injection velocity associated with the weakest cough ($\sim$ 5 m/s peak velocity), compared with the strongest and medium coughs ($\sim$ 20 and $\sim$ 15 m/s, respectively) might prevent the smallest particles from evaporating due to convection effects which leads into a smaller SMD in the ending states of the simulation.

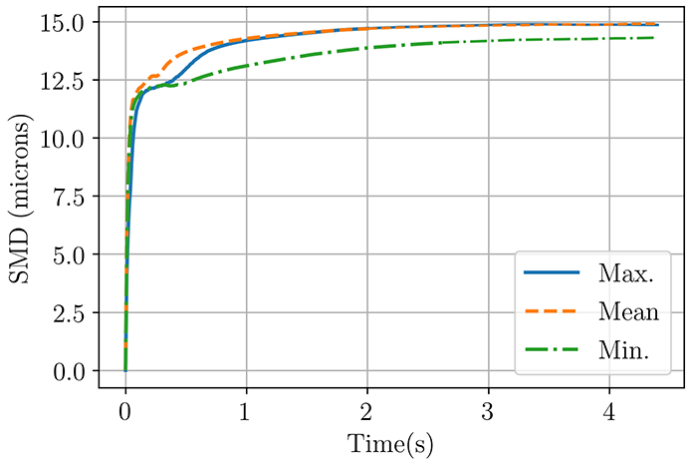

FIG. 10: SMD evolution over time for the three coughs

Payri, R., Martí-Aldaraví, P., Quintero, P. M., Marco-Gimeno, J. (2021). Large Eddy Simulation for the Prediction of Human Coughing. In Atomization and Sprays. https://doi.org/10.1615/atomizspr.2021037129

A further SMD study is assessed by performing a lateral projection of the droplet diameters. The region of interest has been discretized into a domain of 300 $\times$ 300 cells, representing the Y-Z plane. Droplet information has been interpolated into this mesh by analyzing their spatial information (Y and Z coordinates). After that, SMD can be calculated for each cell. It also allows us to observe the evolution of the spray morphology along the time. This procedure has been applied for the strongest and weakest coughs simulated. Results are shown in Figs. 11–13. Differences in penetration and spray shape are coherent with the outcomes obtained in Section 3.1. SMD is uniform spatially along all the spray for the two first instants, while at 0.5 s [Figs. 11(c) and 13(c)] there is a region of low SMD values that links the main spray core with the spray inlet. For the last time instant (1 s), the effect of gravity is observed as a considerable amount of droplets bend their path towards the floor, specially for the jets that have a lower initial momentum [Fig. 11(d)], where the lower part of the spray has a SMD close to 20 micrometers.

The effects of turbulence can also be seen in Figs. 11–13. In the first time instants (0.1 s), the impact of the fluid with the quiescent air generates in its tip a mushroom-like shape. The interaction between phases generates a set of large-scale vortices around the spray body in the shape of a toroid. With increased physical time, the scale of these turbulent structures decreases in size, disintegrating the jet core, generating disturbances, and spreading the droplets around.

3.3 Droplets above Waistline

Cough expelled droplets that remain airborne for long periods of time are of special threat due to the possibility of being an infection source for other organisms. In this study, to distinguish

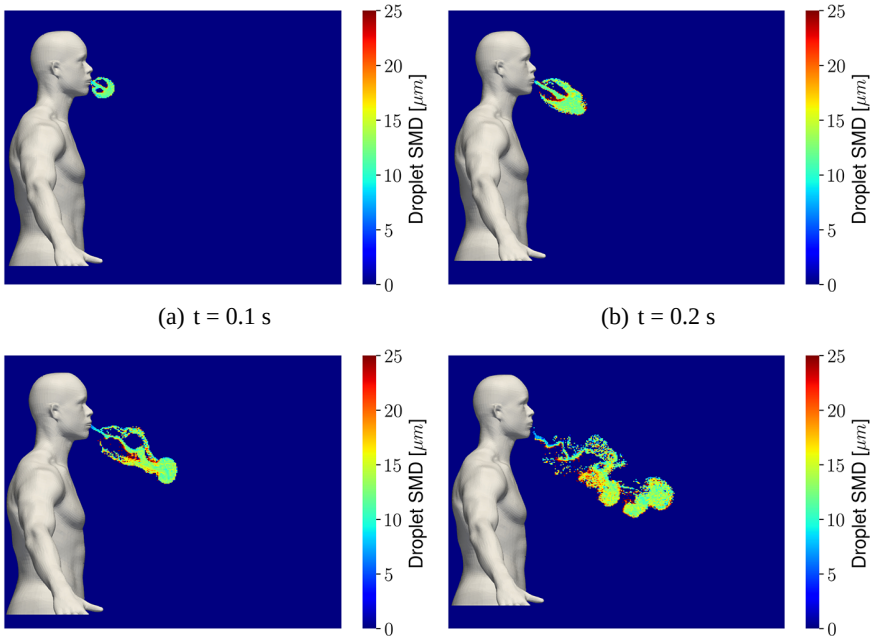

(a) t = 0.1 s (b) t = 0.2 s

(c) t = 0.5 s (d) t = 1 s

FIG. 11: SMD heatmaps at four time instants, for the minimum peak flow rate profile

Payri, R., Martí-Aldaraví, P., Quintero, P. M., Marco-Gimeno, J. (2021). Large Eddy Simulation for the Prediction of Human Coughing. In Atomization and Sprays. https://doi.org/10.1615/atomizspr.2021037129

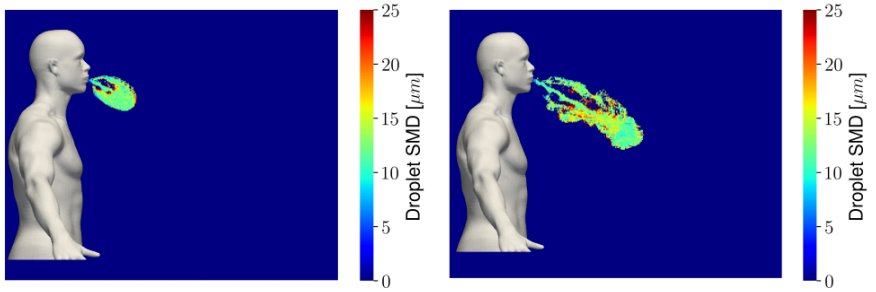

(a) t = 0.1 s (b) t = 0.2 s

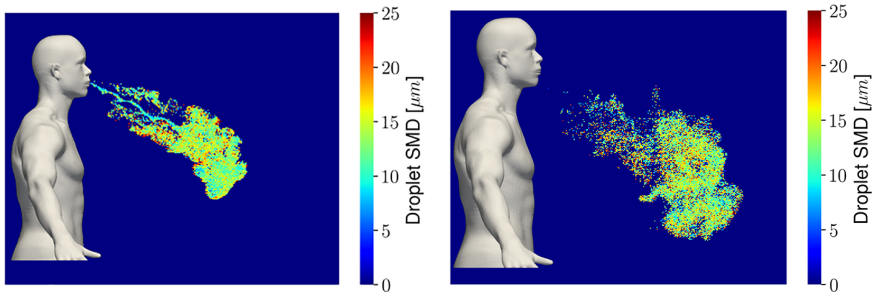

(c) t = 0.5 s (d) t = 1 s

FIG. 12: SMD heatmaps at four time instants, for the mean peak flow rate profile

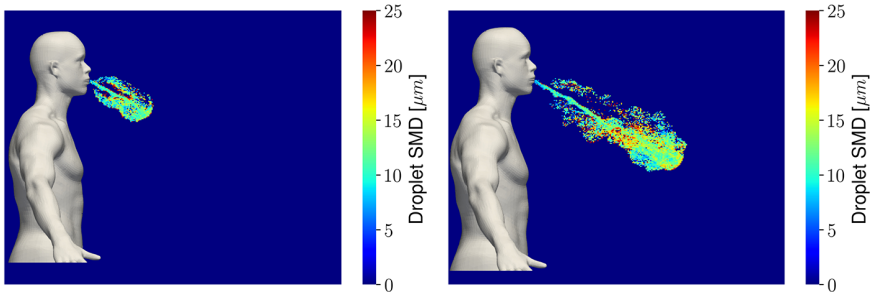

(a) t = 0.1 s (b) t = 0.3 s

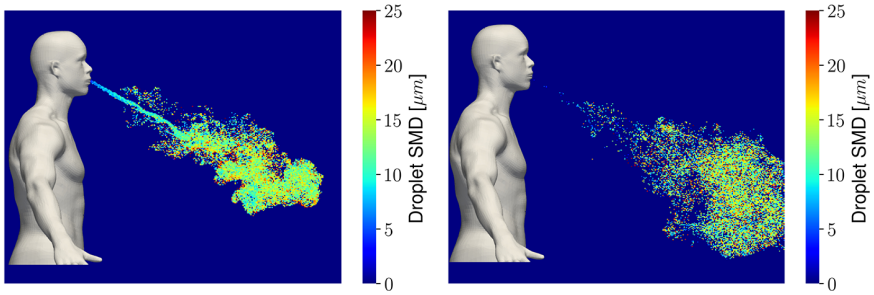

(c) t = 0.5 s (d) t = 1 s

FIG. 13: SMD heatmaps at four time instants, for the maximum peak flow rate profile

Payri, R., Martí-Aldaraví, P., Quintero, P. M., Marco-Gimeno, J. (2021). Large Eddy Simulation for the Prediction of Human Coughing. In Atomization and Sprays. https://doi.org/10.1615/atomizspr.2021037129

between droplets that are of this kind or that have fallen below the human waistline, a threshold height has been defined. This height has been set at 1 m above the ground, and the amount of droplets captured over the time that meet this condition has been plotted. In addition to that, the droplets captured have been discretized according to their diameters to analyze as well the influence of the size. Five diameter thresholds up to the previous value have been used for the mentioned discretization.

Results are presented in Fig. 14 for the three cases simulated. They show how the most frequent droplet found in all three studies falls within the range of 0–5 μm. This differs from the peak value of the RR curve introduced (Fig. 4). This is a consequence of the atomization effects on the spray, as the droplets injected, due to aerodynamic effects, break up into smaller particles. The effect of evaporation, diameter reduction, and droplet breakup affects the 0–5 μm curve, as seen by the oscillations in it. Progressively, the droplets above the specified threshold get reduced whether by droplet size reduction, evaporation, or falling to the ground. Although at larger physical times the percentage of droplets present above the waistline has been reduced, the amount of droplets that remain above it is significant, and the spray continues to be a possible virus spreader. In addition to it, as mentioned, the cough jet is tilted 30° towards the floor, which has an effect on this parameter.

In addition to the amount of droplets of different sizes, it is of interest to study the mass contribution of each range of droplet diameters (Fig. 15). It allows us to obtain how long the

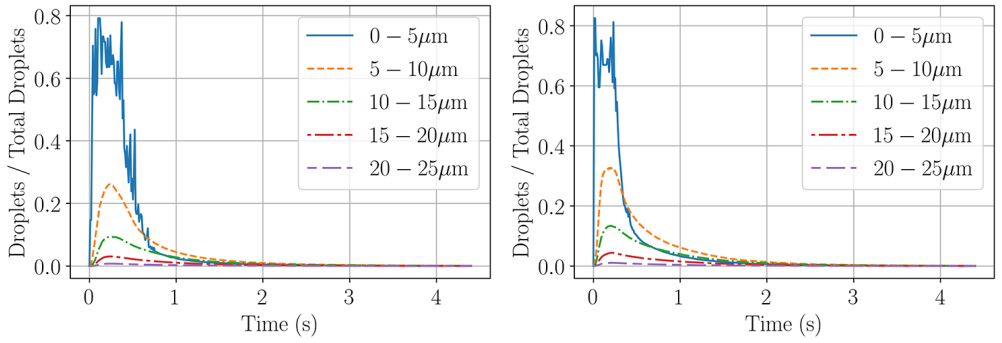

(a) Maximum Flow Rate (b) Mean Flow Rate

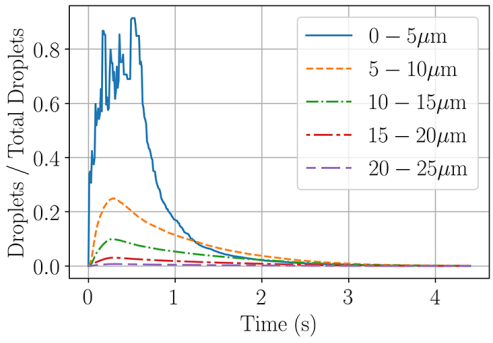

(c) Minimum Flow Rate

FIG. 14: Amount of droplets above 1 m from ground, discretized by its size, for the three coughs simulated

Payri, R., Martí-Aldaraví, P., Quintero, P. M., Marco-Gimeno, J. (2021). Large Eddy Simulation for the Prediction of Human Coughing. In Atomization and Sprays. https://doi.org/10.1615/atomizspr.2021037129

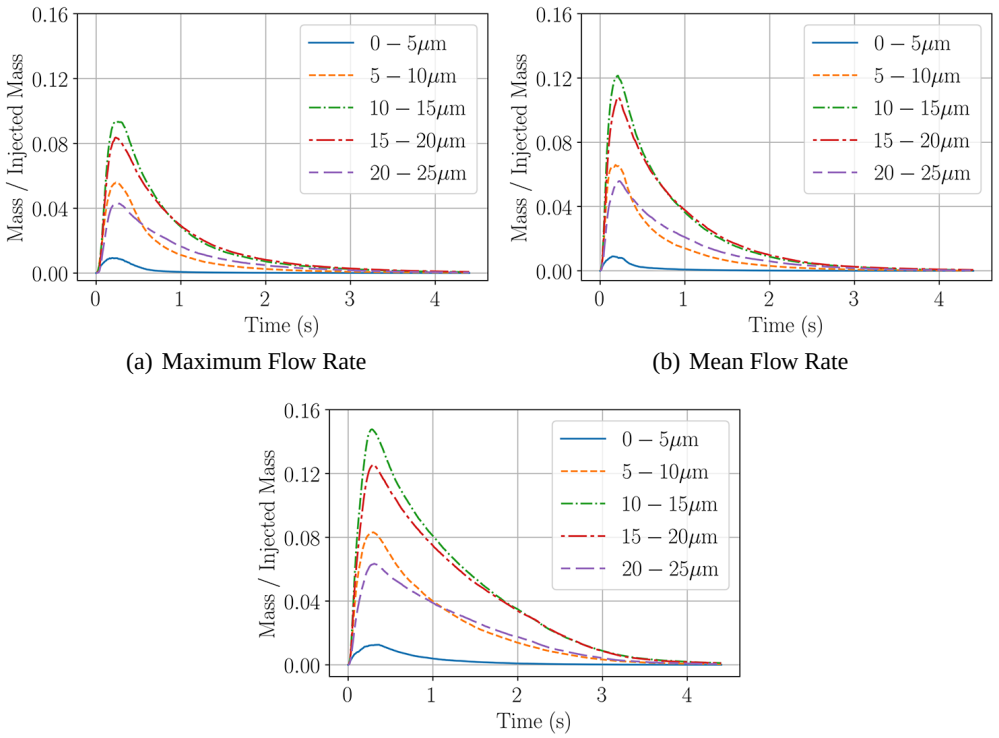

(a) Maximum Flow Rate

(b) Mean Flow Rate

(c) Minimum Flow Rate

FIG. 15: Amount of mass above 1 m from ground, discretized by droplet size, for the three coughs simulated

different droplets stay above the mentioned threshold, without considering the amount of them. Although the amount of small droplets ($D < 5$ μm) is the most common droplet found, it represents the least mass contribution to the total mass injected. The highest mass contribution (10–15 μm) is the most common diameter of Fig. 4. From the curves, it can also be seen how the mass of the small droplets (up to 10 μm) decays in a faster way than large droplets. As the strength of the cough increases (higher inlet velocity), the rate of mass decay due to evaporation and falling to the ground increases, and, as well, the amount of mass present in the domain also decreases. The convective effects enhance the evaporation rate for the stronger cough profiles, while for the weakest cough, the evaporation rate is lower but constant along the time, as seen in Fig. 16.

3.4 Droplet Detection Histogram

From the droplets present at several selected time instants, histograms have been computed to obtain the most common droplet size present at the three cough intensities simulated (Fig. 17). Four time instants have been used to properly capture the two phases the cough consists of (see Section 3.1). All three types of cough follow the same trend. At 0.1 s the distributions are quite similar, followed by a sudden increase in the amount of droplets smaller than 1 μm. This is in concordance with the outcomes from Zayas et al. (2012), which presented a predominance of

Payri, R., Martí-Aldaraví, P., Quintero, P. M., Marco-Gimeno, J. (2021). Large Eddy Simulation for the Prediction of Human Coughing. In Atomization and Sprays. https://doi.org/10.1615/atomizspr.2021037129

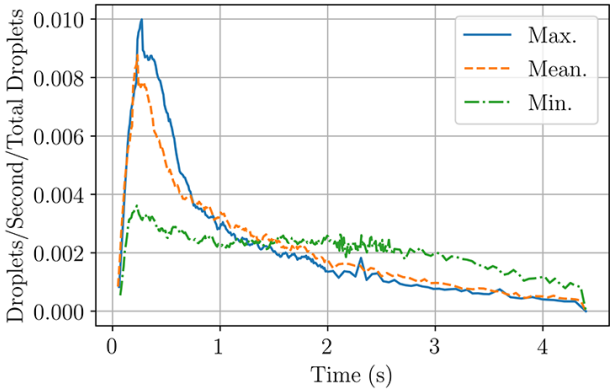

FIG. 16: Evaporation rate of the droplets for the three profiles simulated

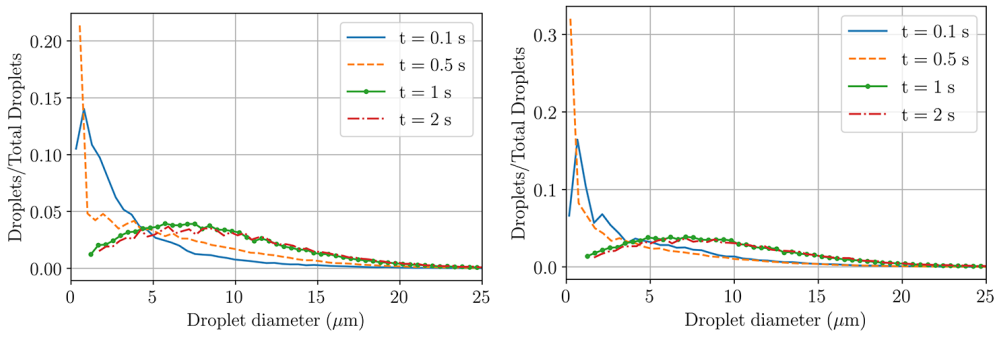

(a) Maximum Flow Rate

(b) Mean Flow Rate

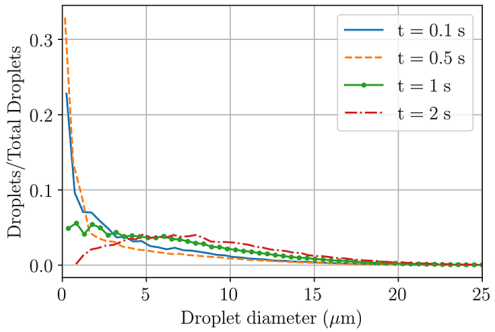

(c) Minimum Flow Rate

FIG. 17: Droplet size probability for different time instants, and for the three cough intensities

diameters of the indicated size. One second after the cough starts, the amount of small particles has decreased for the three simulations, translating the diameter peak towards 12.5 μm. After 2 s, the curve's peak moves barely to higher diameters. This indicates how once the spray has lost its momentum, it remains unaltered in particle size terms; it also indicates the importance of the convective effects on the evaporation, as after this time, the droplet velocities are no longer

Payri, R., Martí-Aldaraví, P., Quintero, P. M., Marco-Gimeno, J. (2021). Large Eddy Simulation for the Prediction of Human Coughing. In Atomization and Sprays. https://doi.org/10.1615/atomizspr.2021037129

important. This is in agreement with the results shown in Fig. 10, which show little variation after the mentioned time.

3.5 Droplet Trajectories

The spatial coordinates of the droplets injected into the gaseous domain have been tracked along their lifeline to detect spread patterns across the air. Figures 18–20 represent the trajectories of the parcels of a certain amount of droplets of each spray. Discretization into particle size has also been applied. Two droplet ranges (0–5 μm and 5–10 μm) have been represented for the sake of clarity. The colors were assigned to each individual droplet injected to follow its path along its lifetime.

The diameter range of 5–10 μm shows generally a smaller amount of droplets during the simulation, which is in concordance with the results of Fig. 14. Additionally, the penetration profiles obtained in Section 3.1 are validated here, as the stronger cough profile reaches further Z coordinates at the end of the simulation. The droplets of all three cases do not fall to the ground, as the minimum Y coordinate at 4 s of physical time did not fall below 0.5 m. Additionally, some of the small droplets [$<$ 5 μm, Figs. 18(a) and 19(a)] tend to ascend after a certain amount of time. This seems to happen on the stronger cough profiles, but not on the weaker one. This is probably due to buoyancy effects, as well as the effect of gravity in the droplets. This indicates

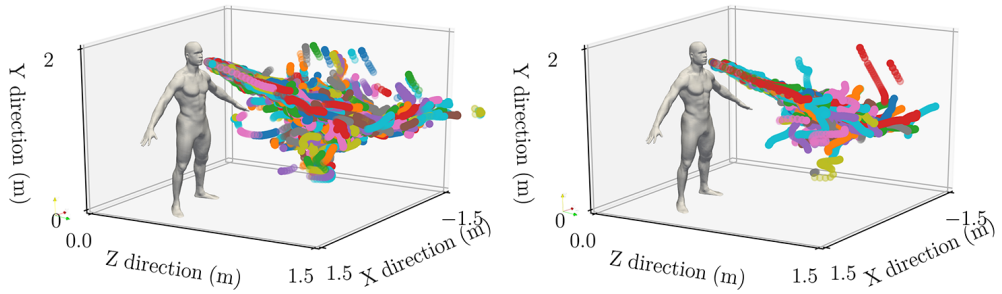

(a) 0–5 μm (b) 5–10 μm

FIG. 18: Evolution of the droplet trajectories, for the different particle diameters found in the spray, for the maximum peak flow rate cough profile

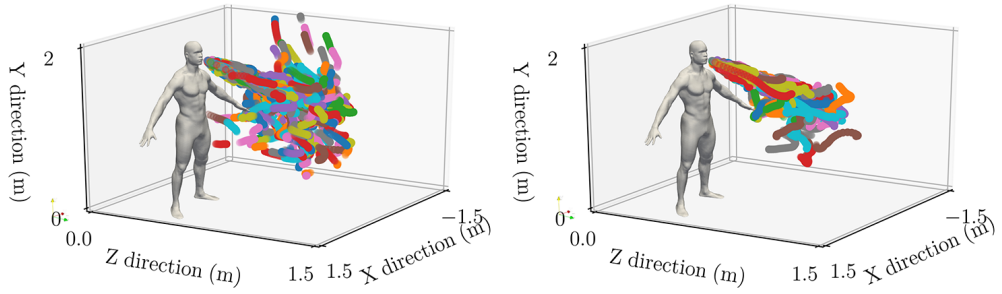

(a) 0–5 μm (b) 5–10 μm

FIG. 19: Evolution of the droplet trajectories, for the different particle diameters found in the spray, for the mean peak flow rate cough profile

Payri, R., Martí-Aldaraví, P., Quintero, P. M., Marco-Gimeno, J. (2021). Large Eddy Simulation for the Prediction of Human Coughing. In Atomization and Sprays. https://doi.org/10.1615/atomizspr.2021037129

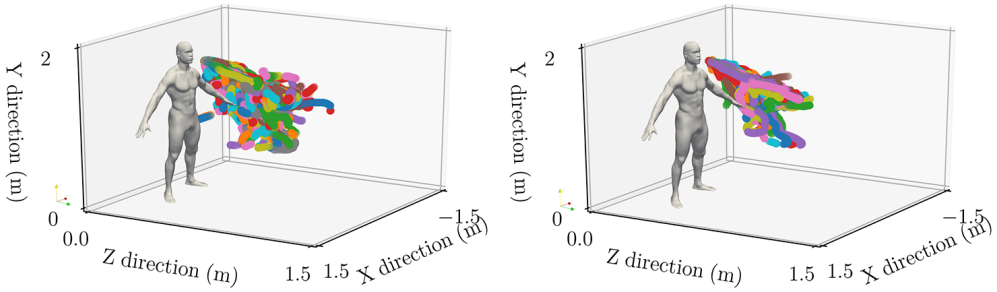

(a) 0–5 μm (b) 5–10 μm

FIG. 20: Evolution of the droplet trajectories, for the different particle diameters found in the spray, for the minimum peak flow rate cough profile

that most of the droplets introduced when coughing, if not evaporated, become airborne, and therefore, potential pathogen transmitters.

In order to detect the reasons behind the lifting of the small droplets, the velocity vector plots have been included for three time instants and the maximum (Fig. 21) and minimum (Fig. 22) peak flow rate cough profile. On the strongest flow rate profile, 0.5 s after the start of the cough event [Fig. 21(a)], toroidal vortex can be observed on the tip of the injected spray, but the droplets stay within the high velocity region. After 1 s [Fig. 21(b)], the toroidal vortex

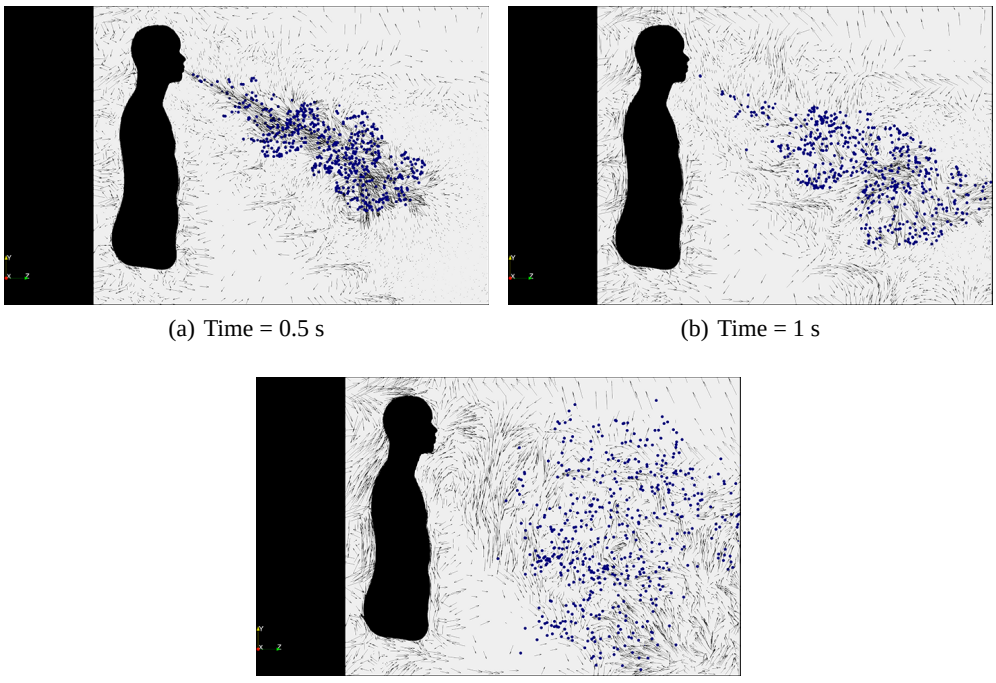

(a) Time = 0.5 s (b) Time = 1 s

(c) Time = 3 s

FIG. 21: Velocity vector plot at three different instants for the strong cough

Payri, R., Martí-Aldaraví, P., Quintero, P. M., Marco-Gimeno, J. (2021). Large Eddy Simulation for the Prediction of Human Coughing. In Atomization and Sprays. https://doi.org/10.1615/atomizspr.2021037129

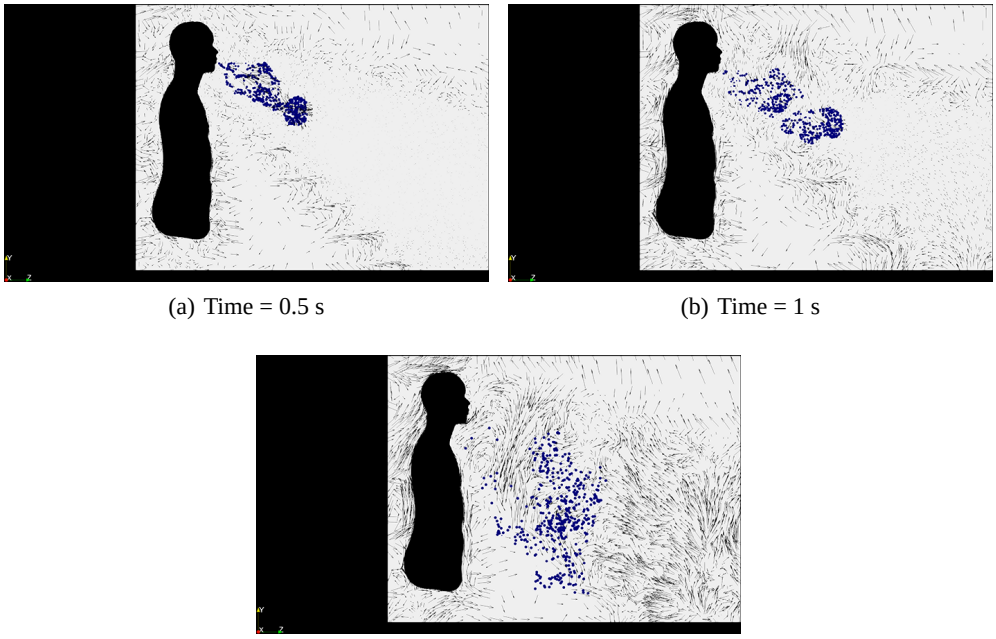

(a) Time = 0.5 s

(b) Time = 1 s

(c) Time = 3 s

FIG. 22: Velocity vector plot at three different instants for the weak cough

is not present anymore; the spray inertia starts to dissipate into the surrounding air, creating recirculating regions capable of moving around the remaining droplets. Three seconds after the cough starts [Fig. 21(c)], these recirculations become more evident and drag the droplets in several directions. On the other hand, the weak profile shows significantly smaller cough velocities. The toroidal vortex can also be found on the spray tip on the initial time instants [Fig. 22(a)]. As it happened on the strong cough profile, it disappears after 1 s. The spray dissipates into recirculating structures, and after 3 s [Fig. 22(c)], the spray has already lost all of its initial inertia. In this case, these structures are considerably weaker than the strong cough profile at 1 s after the injection instant, as in the strong case they are already present after that time. Therefore, the strength of these recirculating structures is the driving reason for finding droplets that start to increase their height. This strength is also tightly related to the cough flow rate profile that represents the cough event.

4. CONCLUSIONS

Due to the recent need to better understand the behavior of human coughs and the droplet distribution, a LES based approach has been followed to obtain characteristic data of human coughing. For it, maximum, minimum, and mean inlet velocity profiles were introduced to model realistic coughs. From them, the following conclusions were obtained:

- The CFD methodology followed predicts for a physical time of 4 s a penetration of 1.75 m for the strongest cough profile simulated. It is expected that longer simulation times will lead to greater penetrations. Weaker coughs penetrate slower. Two penetration phases are

Payri, R., Martí-Aldaraví, P., Quintero, P. M., Marco-Gimeno, J. (2021). Large Eddy Simulation for the Prediction of Human Coughing. In Atomization and Sprays. https://doi.org/10.1615/atomizspr.2021037129

depicted, the first one up to 0.5 s, where the value is driven by the spray initial momentum, and a second phase, where convective flows and buoyancy effects move the spray further down into the domain, in agreement with previous studies.

- SMD does not vary greatly between the cough profiles. Steady values are reached within 2 s, after very small particles are evaporated and bigger ones break up.

- The amount of small particles below 1 μm is predominant in all three cases simulated during the first instants of the injection up to 1 s of physical time, as they account for 60% of the total droplets. The size of these droplets contributes very little to the total mass injected. After 2 s the amount of droplets of all sizes has been greatly reduced, but a considerable amount of droplets remain in the air.

- Vertically, droplets do not fall past a certain height (0.6 m), and some of the small droplets (< 5 μm) even start to increase their height past the injection Y coordinate, indicating that droplets that have not undergone evaporation become airborne.

- Based on the collected data, it seems reasonable to increase the recommended social distancing further than 2 m between people. Penetrations have been found to reach values higher than 1 m and extending the current simulations would increase these values even more.

- Having found that the cough spray dissipates into recirculating regions that keep particles up in the air, and that after enough time, increase their height, forced convective systems such as air conditioning would worsen the situation by introducing turbulent flows that could spread virus transmitter particles further away in the room.

Cough has been shown to be an important virus transmitter due to these later droplets that remain in the air for long times. Social distancing might not be good enough for preventing infection according to these results. This study could be further complemented by altering the ambient conditions, such as humidity, as it will play an important role in the evaporation of water droplets, and therefore the amount of particles that could remain airborne in the air for a long period of time. In addition, due to the high dependency of the droplets' trajectories on turbulent structures, further studies could study the effect of the induced turbulence of air conditioning systems on the transportation of the expelled droplets. Moreover, more expiratory events such as normal human breathing or sneezing could be modeled to analyze minimum interpersonal distances in order to prevent pathogen transmission.

ACKNOWLEDGMENTS

The equipment and resources used in this work have been partially supported by "Conselleria d'Educació, Investigació, Cultura y Esport" of Generalitat Valenciana in the framework of the "Ajudes per a grups d'investigació consolidables" program (Project Reference AICO/2020/208). Additionally, the Ph.D. student Javier Marco-Gimeno has been funded by a grant from the Government of Generalitat Valenciana with reference ACIF/2020/259 and financial support from The European Union.

Payri, R., Martí-Aldaraví, P., Quintero, P. M., Marco-Gimeno, J. (2021). Large Eddy Simulation for the Prediction of Human Coughing. In Atomization and Sprays. https://doi.org/10.1615/atomizspr.2021037129

REFERENCES

Aliabadi, A.A., Rogak, S.N., Green, S.I., and Bartlett, K.H., CFD Simulation of Human Coughs and Sneezes: A Study in Droplet Dispersion, Heat, and Mass Transfer, in *Proc. of ASME Int. Mech. Eng. Cong. Expo. (IMECE)*, vol. **7**, pp. 1051–1060, 2010.

Beale, J.C. and Reitz, R.D., Modeling Spray Atomization with the Kelvin-Helmholtz/Rayleigh-Taylor Hybrid Model, *Atomization Sprays*, vol. **9**, pp. 623–650, 1999.

Bourouiba, L., Dehandschoewercker, E., and Bush, J.W., Violent Expiratory Events: On Coughing and Sneezing, *J. Fluid Mech.*, vol. **745**, pp. 537–563, 2014.

Chao, C.Y., Wan, M.P., Morawska, L., Johnson, G.R., Ristovski, Z.D., Hargreaves, M., Mengersen, K., Corbett, S., Li, Y., Xie, X., and Katoshevski, D., Characterization of Expiration Air Jets and Droplet Size Distributions Immediately at the Mouth Opening, *J. Aerosol Sci.*, vol. **40**, no. 2, pp. 122–133, 2009.

Cole, E.C. and Cook, C.E., Characterization of Infectious Aerosols in Health Care Facilities: An Aid to Effective Engineering Controls and Preventive Strategies, *Am. J. Infect. Control*, vol. **26**, no. 4, pp. 453–464, 1998.

Dbouk, T. and Drikakis, D., On Coughing and Airborne Droplet Transmission to Humans, *Phys. Fluids*, vol. **32**, p. 053310, 2020.

Dudalski, N., Mohamed, A., Mubareka, S., Bi, R., Zhang, C., and Savory, E., Experimental Investigation of Far-Field Human Cough Airflows from Healthy and Influenza-Infected Subjects, *Indoor Air*, vol. **30**, no. 5, pp. 966–977, 2020.

Duguid, J.P., The Numbers and the Sites of Origin of the Droplets Expelled during Expiratory Activities, *Edinburgh Med. J.*, vol. **52**, pp. 385–401, 1945.

Duguid, J.P., The Size and the Duration of Air-Carriage of Respiratory Droplets and Droplet-Nuclei, *J. Hyg.*, vol. **44**, no. 6, pp. 471–479, 1946.

Feng, Y., Marchal, T., Sperry, T., and Yi, H., Influence of Wind and Relative Humidity on the Social Distancing Effectiveness to Prevent COVID-19 Airborne Transmission: A Numerical Study, *J. Aerosol Sci.*, vol. **147**, p. 105585, 2020.

Frössling, N., Evaporation, Heat Transfer, and Velocity Distribution in Two-Dimensional and Rotationally Symmetrical Laminar Boundary-Layer Flow, Tech. Rep. 1432, NACA, 1940.

Gao, N., Niu, J., and Morawska, L., Distribution of Respiratory Droplets in Enclosed Environments under Different Air Distribution Methods, *Build. Simul.*, vol. **1**, no. 4, pp. 326–335, 2008.

Germano, M., Piomelli, U., Moin, P., and Cabot, W.H., A Dynamic Subgrid-Scale Eddy Viscosity Model, *Phys. Fluids A*, vol. **3**, no. 7, pp. 1760–1765, 1991.

Gittings, S., Turnbull, N., Henry, B., Roberts, C.J., and Gershkovich, P., Characterisation of Human Saliva as a Platform for Oral Dissolution Medium Development, *Eur. J. Pharm. Biopharm.*, vol. **91**, pp. 16–24, 2015.

Gupta, J.K., Lin, C.H., and Chen, Q., Flow Dynamics and Characterization of a Cough, *Indoor Air*, vol. **19**, no. 6, pp. 517–525, 2009.

Höppe, P., Temperatures of Expired Air under Varying Climatic Conditions, *Int. J. Biometeorol.*, vol. **25**, no. 2, pp. 127–132, 1981.

Li, X., Shang, Y., Yan, Y., Yang, L., and Tu, J., Modelling of Evaporation of Cough Droplets in Inhomogeneous Humidity Fields Using the Multi-Component Eulerian-Lagrangian Approach, *Build. Environ.*, vol. **128**, pp. 68–76, 2018.

Lipsitch, M., Cohen, T., Cooper, B., Robins, J.M., Ma, S., James, L., Gopalakrishna, G., Chew, S.K., Tan, C.C., Samore, M.H., Fisman, D., and Murray, M., Transmission Dynamics and Control of Severe Acute Respiratory Syndrome, *Science*, vol. **300**, no. 5627, pp. 1966–1970, 2003.

Payri, R., Martí-Aldaraví, P., Quintero, P. M., Marco-Gimeno, J. (2021). Large Eddy Simulation for the Prediction of Human Coughing. In Atomization and Sprays. https://doi.org/10.1615/atomizspr.2021037129

Liu, A.B., Mather, D., and Reitz, R.D., Modeling the Effects of Drop Drag and Breakup on Fuel Sprays, *SAE Int. Congr. Expo.*, vol. **298**, pp. 1–6, 1993.

Liu, S. and Novoselac, A., Transport of Airborne Particles from an Unobstructed Cough Jet, *Aerosol Sci. Technol.*, vol. **48**, no. 11, pp. 1183–1194, 2014.

Loudon, R.G. and Roberts, R.M., Droplet Expulsion from the Respiratory Tract, *Am. Rev. Respir. Dis.*, vol. **95**, no. 3, pp. 435–442, 1967.

Morawska, L., Droplet Fate in Indoor Environments, or Can We Prevent the Spread of Infection?, *Indoor Air*, vol. **16**, no. 5, pp. 335–347, 2006.

Papineni, R.S. and Rosenthal, F.S., The Size Distribution of Droplets in the Exhaled Breath of Healthy Human Subjects, *J. Aerosol Med.*, vol. **10**, no. 2, pp. 105–116, 1997.

Pope, S.B., Ten Questions Concerning the Large-Eddy Simulation of Turbulent Flows, *New J. Phys.*, vol. **6**, p. 35, 2004.

Redrow, J., Mao, S., Celik, I., Posada, J.A., and Gang Feng, Z., Modeling the Evaporation and Dispersion of Airborne Sputum Droplets Expelled from a Human Cough, *Build. Environ.*, vol. **46**, no. 10, pp. 2042–2051, 2011.

Schmidt, D.P. and Rutland, C.J., A New Droplet Collision Algorithm, *J. Comput. Phys.*, vol. **164**, no. 1, pp. 62–80, 2000.

Tang, J.W., Li, Y., Eames, I., Chan, P.K., and Ridgway, G.L., Factors Involved in the Aerosol Transmission of Infection and Control of Ventilation in Healthcare Premises, *J. Hosp. Infect.*, vol. **64**, no. 2, pp. 100–114, 2006.

Tang, J.W., Liebner, T.J., Craven, B.A., and Settles, G.S., A Schlieren Optical Study of the Human Cough with and without Wearing Masks for Aerosol Infection Control, *J. R. Soc. Interf.*, vol. **6**, pp. 727–736, 2009.

Weller, H.G., Tabor, G., Jasak, H., and Fureby, C., A Tensorial approach to Computational Continuum Mechanics Using Object-Oriented Techniques, *Comput. Phys.*, vol. **12**, no. 6, pp. 620–631, 1998.

Xie, X., Li, Y., Sun, H., and Liu, L., Exhaled Droplets Due to Talking and Coughing, *J. R. Soc. Interf.*, vol. **6**, 2009.

Yang, L., Li, X., Yan, Y., and Tu, J., Effects of Cough-Jet on Airflow and Contaminant Transport in an Airliner Cabin Section, *J. Comput. Multiphase Flows*, vol. **10**, no. 2, pp. 72–82, 2018.

Yang, S., Lee, G.W., Chen, C.M., Wu, C.C., and Yu, K.P., The Size and Concentration of Droplets Generated by Coughing in Human Subjects, *J. Aerosol Med.*, vol. **20**, no. 4, pp. 484–494, 2007.

Zayas, G., Chiang, M.C., Wong, E., MacDonald, F., Lange, C.F., Senthilselvan, A., and King, M., Cough Aerosol in Healthy Participants: Fundamental Knowledge to Optimize Droplet-Spread Infectious Respiratory Disease Management, *BMC Pulm. Med.*, vol. **12**, p. 11, 2012.

Zhao, B., Zhang, Z., and Li, X., Numerical Study of the Transport of Droplets or Particles Generated by Respiratory System Indoors, *Build. Environ.*, vol. **40**, no. 8, pp. 1032–1039, 2005.

Zhao, J., Feng, Y., Bezerra, M., Wang, J., and Sperry, T., Numerical Simulation of Welding Fume Lung Dosimetry, *J. Aerosol Sci.*, vol. **135**, pp. 113–129, 2019.

Zhu, S.W., Kato, S., and Yang, J.H., Study on Transport Characteristics of Saliva Droplets Produced by Coughing in a Calm Indoor Environment, *Build. Environ.*, vol. **41**, no. 12, pp. 1691–1702, 2006.